ORP-52758
Revision 0

Rhenium solubility in borosilicate nuclear waste glass: implications for the processing and immobilization of technetium-99

Prepared for the U.S. Department of Energy
Assistant Secretary for Environmental Management

P.O. Box 450
Richland, Washington 99352

Approved for Public Release;
Further Dissemination Unlimited

ORP-52758
Revision 0

Rhenium solubility in borosilicate nuclear waste glass: implications for the processing and immobilization of technetium-99

A. A. Kruger
Department of Energy - Office of River Protection

A. Goel
Pacific Northwest National Laboratory

C. P. Rodriguez
Pacific Northwest National Laboratory

J. S. McCloy
Pacific Northwest National Laboratory

M. J. Schweiger
Pacific Northwest National Laboratory

W. W. Lukens, Jr.
Lawrence Berkeley National Laboratory

B. J. Riley
Pacific Northwest National Laboratory

D. Kim
Pacific Northwest National Laboratory

M. Liezers
Pacific Northwest National Laboratory

P. Hrma
Pacific Northwest National Laboratory

Date Published
May 2012

Royal Society of Chemistry

Published in
Journal of Materials Chemistry

Prepared for the U.S. Department of Energy
Assistant Secretary for Environmental Management

P.O. Box 450
Richland, Washington 99352

Copyright License
By acceptance of this article, the publisher and/or recipient acknowledges the U.S. Government's right to retain a non exclusive, royalty-free license in an to any copyright covering this paper.

Release Approval Date

Approved for Public Release;
Further Dissemination Unlimited

LEGAL DISCLAIMER

This report was prepared as an account of work sponsored by an agency of the United States Government. Neither the United States Government nor any agency thereof, nor any of their employees, makes any warranty, express or implied, or assumes any legal liability or responsibility for the accuracy, completeness, or any third party's use or the results of such use of any information, apparatus, product, or process disclosed, or represents that its use would not infringe privately owned rights. Reference herin to any specific commercial product, process, or service by trade name, trademark, manufacturer, or otherwise, does not necessarily constitute or imply its endorsement, recommendation, or favoring by the Unites States Government or any agency thereof or its contractors or subcontractors. The views and opinions of authors expressed herein do not necessarily state or reflect those of the United States Government or any agency thereof.

This report has been reproduced from the best available copy.

Printed in the United States of America

Rhenium solubility in borosilicate nuclear waste glass: implications for the processing and immobilization of technetium-99

Ashutosh Goel, Brian J. Riley, Martin Liezers, Michael J. Schweiger, Carmen P. Rodriguez, Pavel Hrma, Dong-Sang Kim, John S. McCloy*

Pacific Northwest National Laboratory, Richland, WA 99352, USA

Wayne W. Lukens, Jr.

Lawrence Berkeley National Laboratory, Berkeley, CA 94720, USA

Albert A. Kruger

DOE-WTP Project Office Engineering Division, Richland, WA 99352, USA

Abstract

The immobilization of ^{99}Tc in a suitable host matrix has proved a challenging task for researchers in the nuclear waste community around the world. At the Hanford site in Washington State in the U.S., the total amount of ^{99}Tc in low-activity waste (LAW) is ~1,300 kg and the current strategy is to immobilize the ^{99}Tc in borosilicate glass with vitrification. In this context, the present article reports on the solubility and retention of rhenium, a nonradioactive surrogate for ^{99}Tc, in a LAW sodium borosilicate glass. Due to the radioactive nature of technetium, rhenium was chosen as a simulant because of previously established similarities in ionic radii and other chemical aspects. The glasses containing target Re concentrations varying from 0 to

* Corresponding author Tel.: +1-509-372-4964; Fax: +1-509-372-5997

E-mail address: john.mccloy@pnnl.gov

10,000 ppm by mass were synthesized in vacuum-sealed quartz ampoules to minimize the loss of Re by volatilization during melting at 1000 °C. The rhenium was found to be present predominantly as Re^{7+} in all the glasses as observed by X-ray absorption near-edge structure (XANES). The solubility of Re in borosilicate glasses was determined to be ~3,000 ppm (by mass) using inductively coupled plasma-optical emission spectroscopy (ICP-OES). At higher rhenium concentrations, some additional material was retained in the glasses in the form of alkali perrhenate crystalline inclusions detected by X-ray diffraction (XRD) and laser ablation-ICP mass spectrometry (LA-ICP-MS). Assuming justifiably substantial similarities between Re^{7+} and Tc^{7+} behavior in this glass system, these results implied that the processing and immobilization of ^{99}Tc from radioactive wastes should not be limited by the solubility of ^{99}Tc in borosilicate LAW glasses.

Keywords: radioactive waste; technetium; rhenium; inductively coupled plasma; borosilicate glass

1. Introduction

The Hanford site in Washington is home to approximately 2.1×10^{11} m^3 (~5.5×10^7 gallons) of radioactive and chemically hazardous wastes stored in 177 underground tanks.[1] The wastes were generated as a result of 45 years of plutonium production in support of the nation's defense programs. The current plan is to separate the tank wastes into high-volume, low-activity waste (LAW) and low-volume, high-level waste (HLW) fractions, which will then be vitrified into separate glass waste forms for long-term storage. The LAW vitrification product will be

stored at the on-site integrated disposal facility while HLW glass will be transported to a deep geologic repository when such a location becomes available.[1]

The LAW at Hanford primarily consists of aqueous solutions containing Na^+, K^+, $Al(OH)_4^-$, Cl^-, F^-, NO_2^-, NO_3^-, OH^-, CO_3^{2-}, and organics as well as other minor ionic species, including radionuclides. Some of the main radionuclides found in Hanford LAW include technetium-99 (^{99}Tc), iodine-129 (^{129}I), cesium-137 (^{137}Cs), and strontium-90 (^{90}Sr). The long-lived ^{99}Tc and ^{129}I radionuclides are a matter of concern in comparison to ^{137}Cs and ^{90}Sr, which are short-lived and predominantly fractioned into HLW. According to a recent estimate, the Hanford site tanks contain ~25,000 Ci (~1,500 kg) of ^{99}Tc and ~32 Ci (~180 kg) of ^{129}I.[2] The current flowsheet calculations estimate that more than 90% of the ^{99}Tc inventory in the tanks will be immobilized in the LAW glass whereas only about 20% of the ^{129}I inventory will be incorporated into the LAW glass.[3] According to the performance assessments conducted to provide guidance for the storage and disposal project for Hanford LAW, ^{99}Tc is the major dose contributor during the first 30,000 years following disposal.[2, 4]

The major environmental concern with ^{99}Tc is its high mobility in addition to a long half-life (2.1×10^5 yrs). The highly soluble TcO_4^- does not adsorb well onto the surface of minerals and, thus, migrates nearly at the same velocity as groundwater.[5, 6] On the other hand, the primary concern with processing the Tc-containing waste into a glass is its volatility and hence the low retention.[7] Other sources of Tc-loss may include entrainment with volatilized solvent, formation of aerosols, dust particles in scrubber systems, and other similar sources that can be partially mitigated by engineering systems and recycling.[8] According to the current flowsheet for the Hanford vitrification process, >90% Tc is being estimated to be immobilized in the LAW glass based on the assumption that all the Tc collected through off-gas is recycled back to the

vitrification system. Some recent studies have focused on the issue of Tc volatility from the glass melt with and without cold cap.[9] Partitioning to the molten salt phase has also been suggested as a mechanism for low retention of Tc in the glass.[10] Volatilization of Tc can occur from the salt layer more readily than from the glass, especially if sulfate is present.[11] Therefore, it is critical to understand the mechanism of Tc retention in or escape from glass melt for the management of Tc in LAW vitrification. One of the potential factors that can affect the retention of Tc is its solubility in LAW glass. To the best of authors' knowledge, there is no published data on the solubility of Tc in borosilicate glasses for nuclear waste vitrification. The ultimate goal of the present study is to determine the solubility of Tc in a borosilicate glass for vitrification of Hanford LAW.

Rhenium (Re) has been the preferred non-radioactive Tc surrogate material over other candidates such as Mn or W, because of rhenium's similarities to technetium in chemistry, ionic size, speciation in glass, and other aspects.[8] Although, many studies have reported some differences in the reduction potential of the heptavalent species in Re and Tc,[12-15] the similarities between Re and Tc, as well as ReO_4^- and TcO_4^-, overwhelmingly argue for its utility in obtaining preliminary data which in a non-radioactive environment which can later be corroborated using studies with Tc itself.[15, 16] Rhenium compounds should be chemically similar to those expected for technetium in LAW simulants ($KTcO_4$) as well as those in liquid ($CsTcO_4$, $NaTcO_4$, and $KTcO_4$) and vapor [Tc_2O_7 and $TcO_3(OH)$] phases during vitrification.[8] This paper reports the results on the solubility of Re in a simulated waste glass specifically designed for one of the Hanford's representative LAW streams. The testing with radioactive Tc is in progress and the results will be present in a follow-on article.

2. Experimental

In order to determine the true solubility of Re in a borosilicate glass, the volatilization loss of Re species above the melt was eliminated by heat treating the glasses mixed with Re source material in vacuum sealed (~10^{-4} Pa) fused quartz ampoules so that even the Re species in the gaseous phase would still remain in contact with the glass melt surface. This paper describes the unique experimental procedure designed to perform these solubility experiments along with the results obtained from various characterization techniques in order to quantify the solubility and retention of rhenium in the glasses.

2.1 Glass synthesis

2.1.1 Synthesis of baseline glass

The borosilicate LAW glass with nominal composition shown in Table 1 was synthesized with the melt-quenching technique and is termed the *baseline* glass. The *baseline* glass, or the glass without any Re additions, was made in a large batch from the appropriate amount of oxides (MgO, Al_2O_3, H_3BO_3, SiO_2, Cr_2O_3, ZrO_2, TiO_2, ZnO, Fe_2O_3), carbonates ($CaCO_3$, Na_2CO_3, K_2CO_3) and sulfates (Na_2SO_4). The glass batch was homogenized in a vibrating agate mill and melted in a platinum alloy crucible at 1200 °C for 1 h. The resulting glass was quenched on a steel plate and crushed inside a tungsten carbide mill within a vibratory mixer yielding a fine glass powder.

Table 1. Compositions of the glasses (oxide basis).

Re-conc. (ppm)	Unit	SiO_2	Al_2O_3	B_2O_3	Na_2O	CaO	Fe_2O_3	Cr_2O_3	K_2O	MgO	SO_3	TiO_2	ZnO	ZrO_2	Re_2O_7	$KReO_4$
0	Mass%	45.30	6.10	10.00	21.00	2.07	5.50	0.02	0.47	1.48	0.16	1.40	3.50	3.50	-	-
("baseline")	Mol.%	50.39	4.00	9.60	22.64	2.47	2.30	0.01	0.33	2.45	0.13	1.17	2.87	1.63	-	-
100	Mass%	45.29	6.10	10.00	21.00	2.07	5.50	0.02	0.47	1.48	0.16	1.40	3.50	3.50	-	0.016
	Mol.%	50.39	4.00	9.60	22.64	2.47	2.30	0.01	0.33	2.45	0.13	1.17	2.87	1.63	-	0.004
1,000	Mass%	45.23	6.09	9.98	20.97	2.07	5.49	0.02	0.47	1.48	0.16	1.40	3.49	3.00	-	0.16
	Mol.%	50.37	4.00	9.60	22.64	2.47	2.30	0.01	0.33	2.45	0.13	1.17	2.87	1.63	-	0.04
2,500	Mass%	45.12	6.08	9.96	20.92	2.06	5.48	0.02	0.47	1.47	0.16	1.39	3.49	2.99	-	0.39
	Mol.%	50.34	3.99	9.59	22.62	2.46	2.30	0.01	0.33	2.45	0.13	1.17	2.87	1.63	-	0.09
4,000	Mass%	45.02	6.06	9.94	20.87	2.06	5.47	0.02	0.47	1.47	0.16	1.39	3.48	2.98	-	0.62
	Mol.%	50.31	3.99	9.59	22.61	2.46	2.30	0.01	0.33	2.45	0.13	1.17	2.87	1.62	-	0.14
6,415	Mass%	44.85	6.04	9.90	20.79	2.05	5.45	0.02	0.47	1.47	0.16	1.39	3.47	2.97	-	0.99
	Mol.%	50.27	3.99	9.58	22.59	2.46	2.30	0.01	0.33	2.45	0.13	1.17	2.87	1.62	-	0.23
10,000	Mass%	44.60	6.01	9.84	20.67	2.04	5.41	0.02	0.46	1.46	0.16	1.38	3.45	2.95	-	1.55
	Mol.%	50.20	3.98	9.56	22.56	2.46	2.29	0.01	0.33	2.45	0.13	1.17	2.86	1.62	-	0.36
6,407	Mass%	44.92	6.05	9.92	20.83	2.05	5.45	0.02	0.47	1.47	0.16	1.39	3.47	2.98	0.83	-
	Mol.%	50.33	3.99	9.59	22.62	2.46	2.30	0.01	0.33	2.45	0.13	1.17	2.87	1.63	0.12	-

2.1.2 Synthesis of rhenium containing glasses

Since the predominant form of Tc in the dried Hanford LAW will most likely be an alkali pertechnetate,[8] we chose $KReO_4$ (Alfa Aesar, 99% metal basis, Re 64 mass%) as the primary source of Re for our experiments. In one experiment, Re_2O_7 (NOAH Tech., 99.99%, -4 mesh) was used as an alternative Re-source in order to assess the influence of different Re precursors (with the same oxidation state) on the Re solubility in glass under a controlled environment. The concentration of Re added to the baseline glass was varied between 0 and 10,000 ppm (see Table 1), defined as parts per million, by mass, of Re atoms in the glass. The fractions of the other components in the glasses with Re additions were kept in constant ratios with those in the baseline glass, renormalized to the remaining mass fraction after accounting for the Re-source.

The LAW glass powder (as obtained from the experimental procedure mentioned previously) and the specified amount of Re-source powder were mixed in the tungsten carbide mill to prepare a mixture with a final batch size of 50 g, of which 30 g was used for the Re-solubility study, while the remaining 20 g was set aside for additional experiments. The glass frit was prepared this way so that the sulfate would be well-mixed and soluble in the glass and so that the Re-source powder could be well-mixed within the glass and captured by the glass powder sintering at the maximum allowable solubility. It should be noted that Re-free LAW glass powder (0 ppm Re) was also re-melted under similar conditions and will be considered as the *baseline experiment* in this study.

Each 30 g glass powder batch was placed into a flat-bottomed fused quartz tube and a fused quartz end cap was then inserted into the tube (Fig. 1). The tube was then connected to a vacuum system with compression fitting and evacuated. Once the pressure was ~10^{-4} Pa (~10^{-6} Torr), the tube was sealed with an oxygen-propane torch. This vacuum sealed tube will hereafter

be referred to as the *ampoule*. The ampoule containing powdered glass batch was inserted in the furnace pre-heated at 700 °C. The temperature of the furnace was increased from 700 °C to 1000 °C at a heating rate of 5 °C min^{-1} followed by a dwell of 2 h at 1000 °C to ensure the complete melting of glass batch. Higher temperatures were attempted initially, but there were concerns with 1) dissolving the fused quartz due the high sodium content and thus changing the batch chemistry and 2) having the Re compound attack the ampoule wall. At the end of the heating time, the ampoule containing glass melt was finally quenched in air within a stainless steel canister.

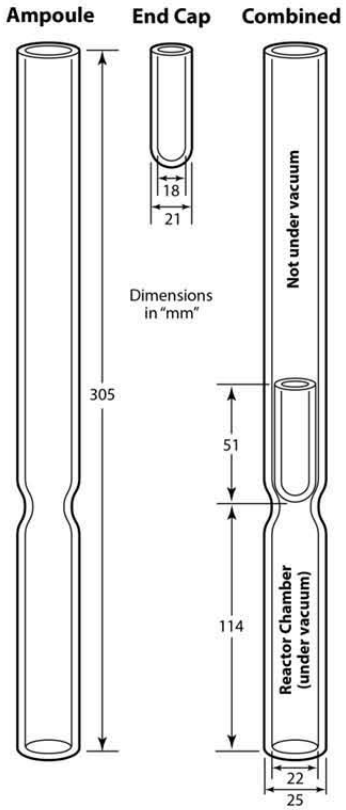

Fig. 1. Schematic of sealed ampoule for glass making. The glass batch is placed in the bottom portion of the combined ampoule on the right.

2.2 Characterization of glasses

2.2.1 X-ray diffraction (XRD)

All of the glasses and selected crystalline samples were analyzed with a Bruker® D8 Advance (Bruker AXS Inc., Madison, WI) XRD equipped with a Cu K_α target at 40 kV and 40 mA. The instrument had a LynxEye™ position-sensitive detector with a scan range of 3° 2θ. Scan parameters used for sample analysis were 5–110° 2θ with a step of 0.015° 2θ and a 0.3-s dwell at each step. In order to obtain higher resolution diffraction data to resolve any additional weak crystalline peaks, the glass samples with Re concentration of 10,000 ppm were analyzed in the 2θ range of 10–60° with a step of 0.015° 2θ and a 2.5-s dwell at each step. For all scans, JADE 6© (Materials Data, Inc., Livermore, CA), software was used to identify phase assemblages.

2.2.2 Scanning electron microscopy-energy dispersive spectroscopy (SEM-EDS)

The microstructure was analysed on select samples with a JEOL scanning electron microscope (SEM, JSM-5900, JEOL Ltd., Tokyo, Japan) equipped with a tungsten filament and a Robinson backscatter electron detector. Additionally, an EDAX Si-drift detector was used to conduct energy dispersive spectrometry (EDS, Apollo XL, AMETEK, Berwyn, PA) for dot mapping. A 20 kV acceleration voltage was used for all imaging and analysis. Note that the baseline glass contained both Si (K_α = 1.739 keV) and Zn (K_α = 8.628 keV) with X-ray emission energies comparable to Re M_α (1.842 keV) and L_α (8.650 keV) X-rays; EDS could not be reliably used for semi-quantitative Re determination.

2.2.3 X-ray Absorption Near Edge Structure (XANES) spectroscopy

For most of the glasses, XANES data were collected at the Re L_2-edge (11959 eV) with the Stanford Synchrotron Radiation Laboratory 11-2 beamline using a Si (220) double crystal

monochromator. The harmonic content of the beam was reduced by detuning the monochromator by 50%. The powdered glass samples were contained in aluminum holders sealed with Kapton tape. Data were recorded in transmission mode using Ar-filled ion chambers or in fluorescence mode using a 32-element Ge detector and were corrected for detector dead time effects. Data analysis was performed by standard procedures[17] with Artemis software.[18] The Re XANES spectra were also analysed by principal component analysis with SixPack software.[19]

Reference spectra for ReO_2, ReO_3 and $KReO_4$ were used for data fitting. The data fitting was based on a non-linear least squares method and was performed in the locally written program "fites." Six parameters were used in the fit: the amplitudes of the three standards, one global energy shift, and slope and offset (linear correction to account for differences in background correction). Data were fitted between 11940 and 12040 eV and the data resolution is estimated to be 6.5 eV based on the width of the white line at the Re L_2-edge. The actual improvement of the fit due to incorporation of the ReO_2 and ReO_3 standards was examined with an F-test by comparing χ-squared with and without the ReO_2 standard. The null hypothesis in the F-test was that including the additional rhenium oxide spectrum did not improve the fit, and a probability of F, or p(F), is less than 0.05 indicating that inclusion of a fraction of the particular rhenium oxide spectrum improved the fit to better than two times the standard deviation. No F-test was performed on the $KReO_4$ standard as this was the main component in all spectra. Additional data on the goodness-of-fit are included in the **Supplementary Information**.

2.2.4 Laser ablation-inductively coupled plasma-mass spectrometry (LA-ICP-MS)

The LA-ICP-MS was used to analyze the chemical nature of bulk (polished) glass samples and to detect the presence of any crystalline/metallic Re inclusions in the samples. Glass samples were embedded in resin and polished to a 1-μm finish prior to LA-ICP-MS analysis.

The polished glass samples were mounted in a laser system sample holder (UP-266 Macro, New Wave Research Inc, USA) and coupled to a quadrupole ICP-MS (PQ Excell, VG Elemental, England). The rhenium sensitivity for ^{187}Re was ~1,000 counts per second per ppm (cps/ppm), based on a raster ablation with a 20-μm diameter laser spot, rising to ~8,200 cps/ppm with a 70-μm diameter laser ablation spot. These values were determined by ablating the National Institute of Standards and Technology (NIST) "50 ppm" trace elements in a Standard Reference Material (SRM) 612 glass standard.[20] Additionally, comparative measurements were made with the "500 ppm" trace elements in glass standard SRM 610.[20] These standards are not certified for Re concentration, but have been measured by dissolution methods and reported in the literature, with SRM glass number 612 having 6.57 ppm Re content and SRM glass number 610 having 49.9 ppm Re content.[21]

Rhenium distribution studies on the fabricated glasses were performed by ablating a grid of 100 spots, typically 0.5 × 0.5 mm total area, repeating the measurement over five to six sites across a sample and averaging the data. Single point feature studies such as probing intact gas bubbles were performed by allowing the laser to ablate into the glass to reach the subsurface feature of interest. For these types of analysis the ICP-MS was run in time-resolved analysis mode. More details on the depth profiling with LA-ICP-MS is provided in the **Supplementary Information**.

During Re analysis, the laser was scanned over the surface of the sample in a raster pattern (scan speed 25 μm/sec) for a period >3 minutes while the ICP-MS collected the intensities of target analytes averaged over three one-minute blocks. Similar laser ablation measurements were performed on the SRM 612 and/or SRM 610 standards under identical conditions and the Re levels in the test glasses were estimated by relative signal ratios assuming

the reported Re concentration in these standards as stated above. These SRM glasses were run before and often in the midst of the unknown Re concentration glasses each day that the LA-ICP-MS was run to account for variations in set-up, laser power drift, and other uncontrolled factors.

2.2.5 Inductively coupled plasma-optical emission spectroscopy (ICP-OES)

The ICP-OES was employed to quantify the Re concentration (irrespective of its solubility or retention) in the as-synthesized glasses. Fragments of glass samples weighing 20–40 mg were dissolved in 2 mL of concentrated ultra-pure (Optima Grade, Thermo-Fisher Scientific, Canada) hydrofluoric acid (HF) by mild heating (no boiling) at ~ 100 °C on a hot plate in 15 mL, capped perfluoro-alkoxy (PFA) crucibles for 2–3 hours. This procedure left a small amount of undissolved white powder. The bulk Si was then slowly evaporated off with the HF until it was completely dry. Then, 2 mL of concentrated hydrochloric acid (HCl) was added and evaporated. Then, a mixture of 0.5 mL HCl and 1.5 mL HNO_3 was added to the PFA crucible and heated gently for 1 h.

Once the glass dissolution was completed and the crucible was allowed to cool down to room temperature, the contents of each crucible and 18.2 Megaohm deionized water rinses were transferred to weighed test tubes yielding ~10 g of total solution. From this solution, a weighed volume was further diluted by a factor of ten using 1% by mass HNO_3 to prepare the final solution for ICP-OES analysis (ICAP 6500 Duo, Thermo-Fisher Inc., England). Typical sample Re concentrations were in the range 0.1–2 ppm after final dilution. Quantitative analysis was performed by generating a calibration curve at three Re emission wavelengths (197.3, 221.4 and 227.5 nm), by serial mass dilution of a Re 999 ± 2 ppm solution concentration standard (Inorganic Ventures, USA) in 2% by mass HNO_3. The calibration plots for all three wavelengths showed a linearity of 0.99 or better.

3. Results and discussion

3.1 Structural characterization of glasses

Melting the initial glass frit at 1200 °C for 1 h was sufficient to produce a homogenous baseline (no Re) LAW glass with dark brown color. The absence of crystalline inclusions was also confirmed by XRD and SEM analyses. The glass transition temperature (T_g) determined from the DSC thermograph for this glass was ~530 °C while no exothermic crystallization curve could be observed until 1100 °C (see **Supplementary Information**). Magic angle spinning-nuclear magnetic resonance (MAS-NMR), Fourier transform infrared (FTIR) spectroscopy, and Raman spectroscopy were also conducted to characterize glasses as a function of Re source additions. Details of these measurements can be found in the **Supplementary Information**. In general, these techniques showed a glass composed of primarily Q^2 and Q^3 structural units, with Si, Al, or B tetrahedra, due to the large sodium content causing non-bridging oxygens. Aluminum is 4-coordinated, and boron is largely 3-coordinate with some 4-coordinated. Rhenium source additions did not appear to have clear effects on the glass structure as evidenced by MAS-NMR, FTIR, and Raman spectroscopy. Thus at the concentrations that remain in glass, the Re appears to be neither a glass-former nor a strong glass modifier. As discussed below, it likely exists in isolated ReO_4^- anions in the interstices of the glass network.

3.2 Crystallinity in Re glasses

The rhenium-containing glass melts exhibited different physical and chemical features during the glass synthesis depending on their initial rhenium concentration. A brief account of visual observations that were made during synthesis of these glasses along with the results obtained from characterization of these glasses by XRD and SEM-EDS is presented below.

Remelting of the baseline glass (with 0 ppm Re) in the quartz ampoule resulted in a cylindrical shaped glass ingot, which cracked and shattered into small pieces upon cooling due to the stresses from a thermal expansion mismatch between the glass and fused quartz. No significant interfacial reactions between glass melt and walls of quartz ampoule were observed. The addition of Re (100–2500 ppm) in the baseline glass with $KReO_4$ as its source resulted in amorphous glasses as revealed by XRD analysis (Fig. 2). Further increase in the Re concentration to ~6400 ppm (source: $KReO_4$) led to the formation of a separate low viscosity liquid phase (estimated to be < 0.1 Pa s) floating on top of the glass surface during cooling that gradually solidified to a white-colored superficial powdered layer. The XRD analysis of this superficial white powder revealed its highly crystalline nature with the dominance of alkali perrhenates along with some minor phases, notably sulfates (Fig. 3), while the glass itself remained amorphous (Fig. 2). Similar observations were made for the glass with 10,000-ppm Re (source: $KReO_4$) where a low viscosity liquid phase floated on the top of the glass and gradually solidified to form a highly crystalline white powder on the surface of the solidified glass. This powder was identified as having a dominance of $NaReO_4$ phase along with some minor phases including $KReO_4$ plus SiO_2, the latter likely due to impurity addition from the walls of quartz ampoule (Fig. 3).

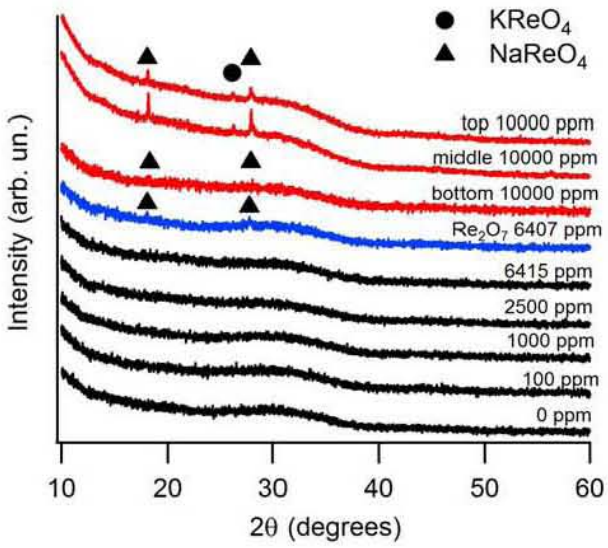

Fig. 2. Powder XRD of glasses.

Unlike the 6,415 ppm (source: $KReO_4$) sample which exhibited no crystalline peaks, the glass obtained with the 10,000 ppm Re concentration showed evidence of $KReO_4$ and $NaReO_4$ phases. In order to obtain an insight into the distribution of crystalline inclusions in the sample, the glass was cut in three sections (bottom, middle, top) relative to the cooled white salt phase. The powder XRD analysis on three different parts of the glass sample revealed the heterogeneous distribution of crystalline inclusions of alkali perrhenates in the sample as the top and middle sections of the glass exhibited the strong crystallinity while the bottom section of glass was only weakly crystalline (Fig. 2). The explanation for this spatial segregation of crystalline phases is not clear, but it may be related to the transport of supersaturated rhenium towards the surface in bubbles where eventually forms a surface salt phase.

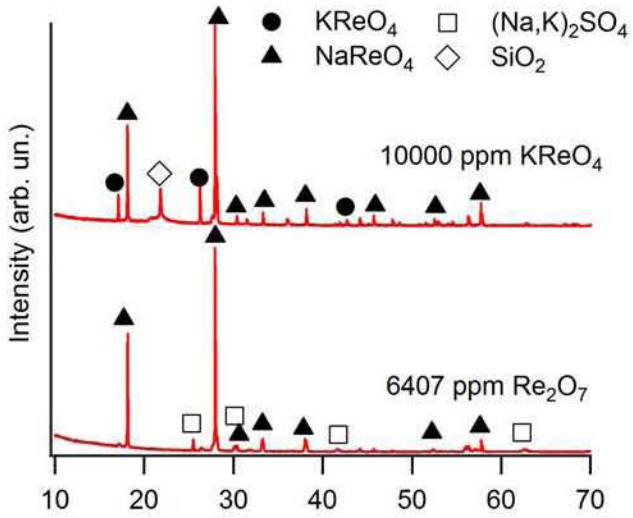

Fig. 3. XRD of white salt from melt surface.

With respect to the synthesis of glass with Re_2O_7 as the rhenium source and Re concentration of ~6,400 ppm, we did not observe any significant interaction between the glass melt and walls of the quartz ampoule. From XRD analysis, the resulting glass did show Re-containing crystalline phases (Fig. 2) similar to the 10,000 ppm $KReO_4$ sample. Also similar to its $KReO_4$ containing counterpart, a low-viscosity liquid phase was observed floating on the top of the glass surface that gradually solidified to white-colored superficial powdered layer. The XRD analysis of the white powder revealed its crystalline nature (Fig. 3) with $NaReO_4$ as the major crystalline phase with minor phases of $KReO_4$ and alkali sulfate. The bottom part of the quartz ampoule cracked after a few minutes of air-quenching due to the thermal stresses, leading to the release of a plume of gas in the canopy hood above the furnace.

The SEM micrographs of the white powder at different locations on the glass surface illustrate their highly crystalline microstructure with dendritic morphology as shown in Fig. 4. The EDS elemental dot mapping of the dendritic crystals found on a fracture surface reveals the dominance of sodium, sulfur and rhenium in these crystals (Fig. 5). It is noteworthy that,

although the crystalline microstructure of the white powders is enriched in sulfur along with Re and Na, we did not observe any Re-S containing phase during the XRD analysis (Fig. 3). Additionally, the EDS confirms that the sulfur is associated with sodium (probably Na_2SO_4 with some K), while the rhenium appears to be mostly associated with potassium (probably $KReO_4$ with some Na). It is likely that the perrhenate and sulfate salts were intimately mixed in the low viscosity liquid on top of the glass and then deposited in the crack upon cooling where they formed separate crystalline phases.

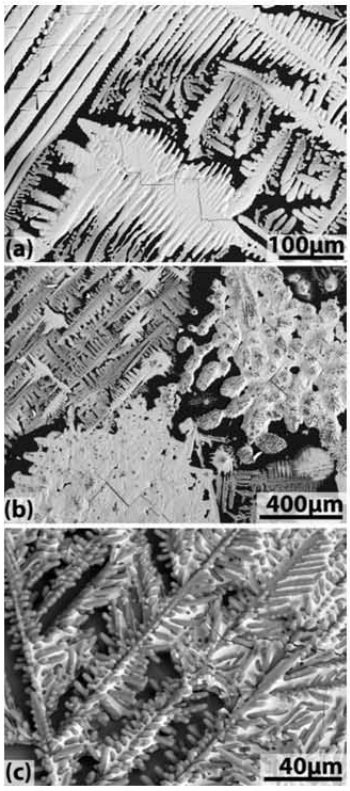

Fig. 4. SEM micrographs of salt phase on the top (a,b) and fracture surfaces (c) of the Re_2O_7 glass.

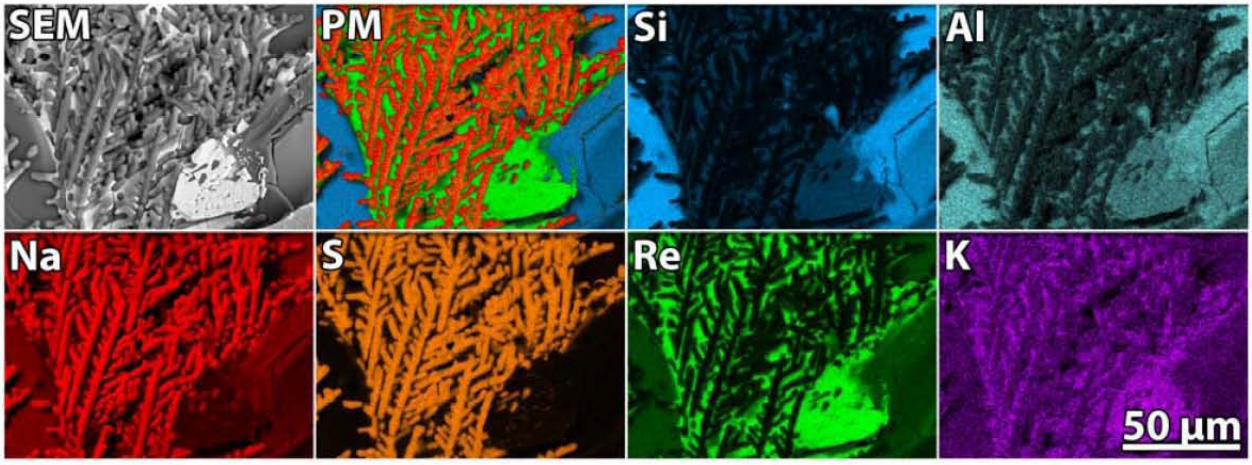

Fig. 5. Backscattered electron SEM micrographs, phase map (PM), and elemental distribution (Si, Al, Na, S, Re, and K) for dendritic crystals found on the fracture surface of the Re_2O_7 glass (based on results from EDS analysis).

3.3 Rhenium valence and coordination in glasses

The Re-XANES spectra of the studied glasses are presented in Fig. 6 while the fitting results are presented in Table 2. Fitting results of glasses at the two extremes of Re loading are shown in Fig. 7. The F-test revealed that the ReO_2 and ReO_3 standards do not significantly improve the fit for any of the glass samples since p(F) in all cases is greater than 0.05. However, for glass prepared with 10,000 ppm $KReO_4$, the amount of Re^{7+} is not within two standard deviations of 1.0, and it is possible that other, lower valent Re species are present in this sample. These results are in general agreement with those reported by Lukens *et al.*[12] which predicts only Re^{7+} at these oxygen fugacities. However, the 10,000 ppm result in this work suggests that this sample may contain other Re species as well, but even if so, the Re^{7+} accounts for 90% of the Re species and so is of primary importance.

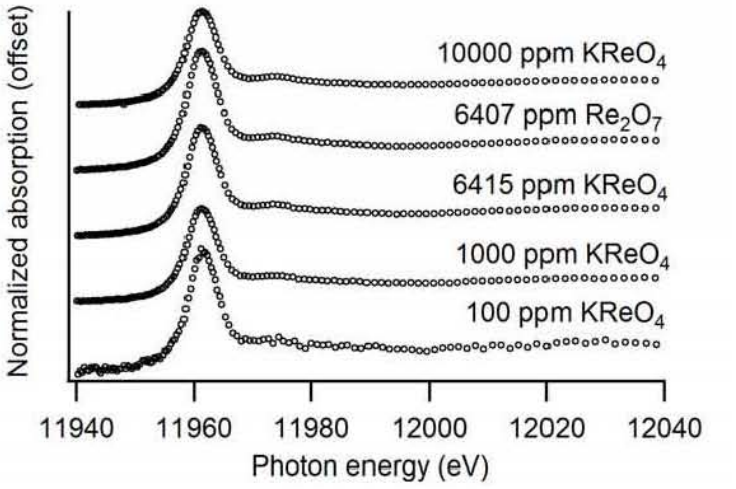

Fig. 6. XANES results for some of the glasses (data are offset for clarity).

Table 2. XANES fitting results.

ppm Re target	Re source	ReO_2*	p(F)†	ReO_3*	p(F)^	$KReO_4$*
100	$KReO_4$	0.0(2)	1.00	0.0(2)	1.00	1.0(1)
1000	$KReO_4$	0.03(9)	0.77	0.03(8)	0.72	0.94(5)
6415	$KReO_4$	0.04(7)	0.61	0.04(6)	0.60	0.93(4)
10000	$KReO_4$	0.09(6)	0.23	0.03(5)	0.63	0.89(3)
6407	Re_2O_7	0.05(7)	0.55	0.05(6)	0.51	0.91(4)

* Number in parentheses is the standard deviation and is in the same units as the digit preceding it.
†p(F) is the probability that the improvement in the fit due to adding this component is due to random error. The component can be considered present in the sample if p(F) is less than 0.05.

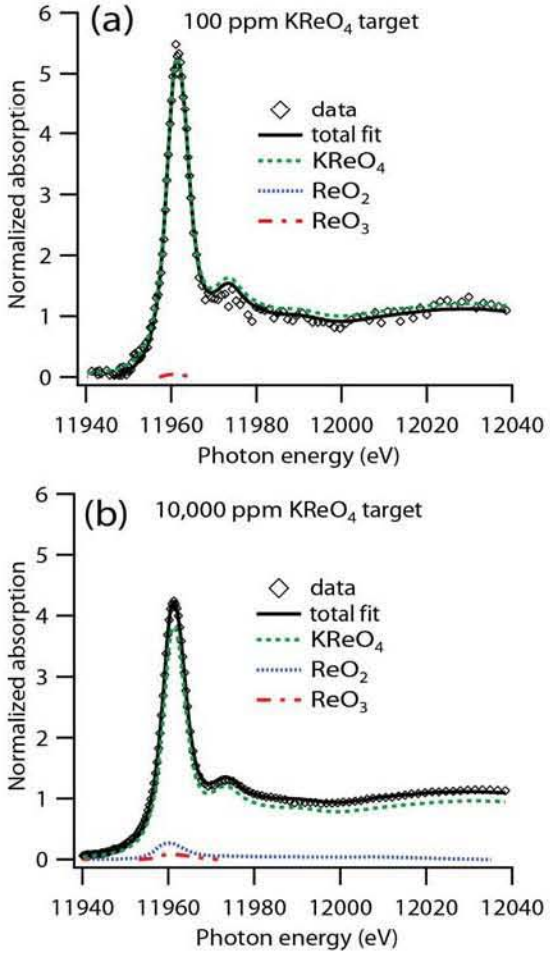

Fig. 7. Fitted XANES data for (a) 100 ppm and (b) 10,000 ppm $KReO_4$ glasses.

3.4 Rhenium solubility in glasses

In agreement with the XRD results (Fig. 3), the presence of rhenium-rich crystalline inclusions in the glass with target Re concentration 6,415 ppm (source: Re_2O_7) was confirmed by LA-ICP-MS data as presented in Fig. 8. A sharp increase in the intensity counts for ^{187}Re in Fig. 8 imply that the laser beam ablated a Re-containing crystalline inclusion that was likely in the form of $NaReO_4$ as detected by XRD analysis (Fig. 3). The depth profiling process used to distinguish bubbles from inclusions is described in the **Supplementary Information**.

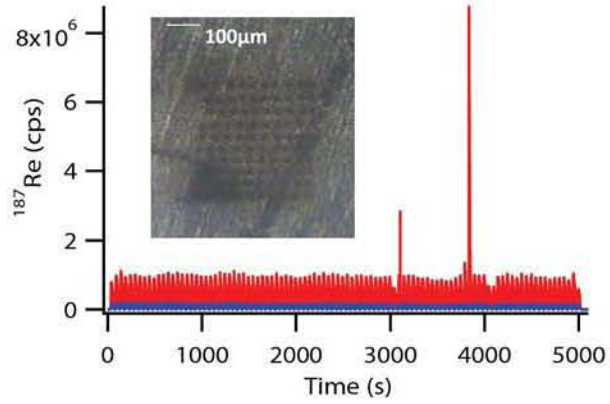

Fig. 8. LA-ICP-MS signal versus time, showing the presence of Re inclusions in the 6407 ppm Re glass made with Re_2O_7. Inset shows typical ablation pattern. The blue background signal (very low counts) is ^{96}Zr for comparison.

Quantitative ICP-OES results are shown in Table 3. Each glass was sampled at least twice and up to six times where various locations in the glass ingot were studied. Heterogeneity in the Re_2O_7 glass and 10,000 ppm $KReO_4$ glass was further confirmed by ICP-OES taken from different regions of the sample (top, middle, or bottom) (Fig. 9). ICP-OES analysis on the different pieces of glass revealed the higher concentration of rhenium in the top and middle parts of the glass sample in comparison to the bottom part of sample, which is in agreement with the result of higher crystallinity in the upper parts of the sample, and may be due to details of the transport of supersaturated rhenium to the surface of the melt such as in bubbles. Similar results

were obtained for the glass with 10,000 ppm of target Re concentration (source: $KReO_4$) as ICP-OES showed that the experimental rhenium concentration varied between 3000 and 4000 ppm in different pieces of glasses. These results are in good agreement with the XRD results presented in Fig. 3. By contrast, the 4,000 ppm (source: $KReO_4$) glass, produced last as a test case, showed relatively uniform Re concentration ~3000 ppm in all portions of the glass.

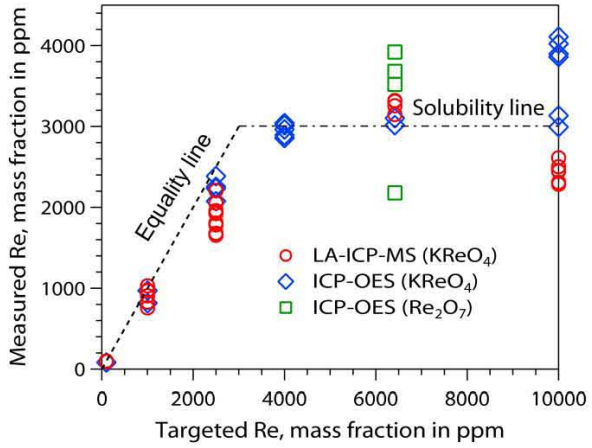

Fig. 9. Quantitative assessment of Re solubility in borosilicate glass

Table 3. ICP-OES results.

Target Re-conc. (ppm)	Re-Source	Location	Sample 1 (ppm)	Sample 1 Std. Dev (ppm)	Sample 2 (ppm)	Sample 2 Std. Dev (ppm)	Overall Mean (ppm)	Overall Std. Dev (ppm)	Inclusions*
100	$KReO_4$	n.t.	38	5	82	12	60	9	N
1000	$KReO_4$	n.t.	971	14	815	13	893	14	N
2500	$KReO_4$	Top	2075	67	2233	60	2154	64	N
		Bottom	2252	55	2385	47	2319	51	N
4000	$KReO_4$	Top	3042	41	3035	42	3038	41	N
		Middle	3013	44	2890	41	2952	43	N
		Bottom	2963	38	2856	40	2909	39	N
6415	$KReO_4$	n.t.	3016	23	3102	30	2059	27	N
10000	$KReO_4$	Top	3897	17	3859	21	3878	19	Y
		Middle	4021	19	4108	19	4065	19	Y
		Bottom	2993	12	9194	15	3064	14	Y
6407	Re_2O_7	Top	3681	25	3920	31	3801	28	Y
		Bottom	2178	19	3520	28	2849	24	Y

*"N" means that inclusions were not observed and "Y" means that inclusions were observed with XRD and/or LA-ICP-MS

n.t. – not tracked

Individual mean and standard deviation is determined from evaluation of four Re absorption lines for each sample. Overall mean and standard deviation is determined based on mean of the statistics of two independent samples. Data are rounded to the nearest ppm.

LA-ICP-MS data should be considered semi-quantitative, as proper quantification depends strongly on choosing a proper standard with the element of interest in the right range within a matrix that ablates similarly to the unknown sample.[22] The SRM glasses had very low Re concentration and gave unreasonably low numbers when used as the only source of calibration. Therefore, we chose to scale the LA-ICP-MS to the truly quantitative ICP-OES data as follows. The average value of the LA-ICP-MS results obtained using the SRM for 100, 1,000, 2,500, and 6,415 ppm $KReO_4$ samples was plotted against the average ICP-OES results for these same glasses and a scale factor of 1.798 was found to be reasonable to apply to the LA-ICP-MS individual values. As an independent check, two samples were analysed with electron probe microanalysis with wavelength dispersive spectroscopy (EPMA-WDS) and the quantified trend followed for variation in rhenium concentration in glasses is similar to that observed for the data obtained from ICP-OES and LA-ICP-MS (see **Supplementary Information**).

The ultimate solubility of Re in the borosilicate LAW glass (shown in Fig. 9) was determined as follows. The quantitative data from 4,000 ppm target (6 data points), 6,415 ppm target $KReO_4$ source (2 data points), and 10,000 ppm (2 data points with lower values) were averaged to obtain a value of 3,004 ppm. The justification for using the two lower values of the 10,000 ppm sample was that these points likely represented the bulk glass, whereas the two points with the higher Re measured values likely contained Re salt inclusions resulting in larger measured Re concentrations. The results of this analysis are shown in Fig. 9, which is considered the key result of our work. Here the "equality line" is shown representing where solubility is equal to retention of the Re, and the "solubility line" is shown representing the maximum incorporation of Re in the glass under these conditions without forming inclusions.

3.5 Rhenium retention in glasses

'Solubility' is defined as the concentration (in mass fraction) of Re at an established equilibrium between dissolved and atmospheric Re. However, the glass-making process generally does not allow the glass melt to reach equilibrium. While the portion of a component dissolved in the amorphous phase(s) may be unsaturated (i.e. below the solubility), a substantial portion may simultaneously exist in the form of inclusions (i.e. inhomogeneities). Therefore, the retention ratio is a dynamic quantity that depends on the glass-making conditions.[23] The retention ratio for of a particular element, *i*, is defined as

$$R_i = \frac{g_{i,r}}{g_{i,0}} \quad (1)$$

where $g_{i,0}$ is the target mass fraction of the element *i* (Re in present case) in the glass (i.e., the mass fraction of Re that would be present in glass if the total amount added with the feed were retained) and $g_{i,r}$ is the mass fraction of rhenium actually retained in the glass (here, as determined by ICP-OES analysis) and since $g_{i,0} \geq g_{i,r}$, $R_i \leq 1$. The difference between $g_{i,0}$ and $g_{i,r}$ is caused by losses to the atmosphere due to volatility and by the formation of surface salt phase enriched with Re. In an actual glass melter application, the retention is strongly influenced by volatility, which is enhanced when there is no cold cap present where unconverted feed covers at least part of the melt surface. Fig. 10 presents the retention ratio for Re in the investigated glasses. The following observations can be made from the obtained results:

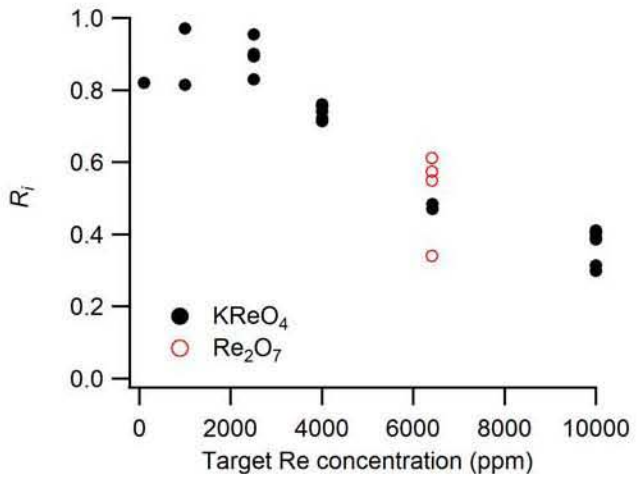

Fig. 10. Retention ratio, R_i, as a function of Re source input concentration.

- The Re concentration in glasses as obtained from ICP-OES varies almost linearly with the target Re concentration in the range of 100–2500 ppm as shown in Fig. 9. This shows that most of the rhenium (80–90%) added to the borosilicate glasses has been retained, the rest presumably being lost to volatilization. Further, the absence of any crystalline inclusions in these glasses confirms that at least up to 2,500 ppm Re concentration, retention ≤ solubility.
- An increase in the target Re concentration beyond 2,500 ppm led to the deviation in retention behavior from linearity. The maximum amount of Re retained in glass with target Re concentrations of 6,415 ppm (source: $KReO_4$) and 10,000 ppm were ~3,000 ppm and 3,000–4000 ppm, respectively. In the latter case, the 4,000 ppm was likely due to the presence of inclusions.
- The difference in Re-precursors (Re_2O_7 versus $KReO_4$) used in the glass melting showed its effect on Re-retention. Though two glasses were made at similar Re target levels of ~6400 ppm, the Re_2O_7 containing glass exhibited Re-concentration of 2,100–4,000 ppm (see Table 3), 3324±782 ppm by ICP-OES for four samples, while a much more repeatable ~3,000 ppm

Re, 3059±61 ppm by ICP-OES for two samples, was detected for $KReO_4$ glass (Fig. 9). Note that although fewer ICP-OES samples were investigated for the $KReO_4$ glass of this target Re concentration, multiple samples of LA-ICP-MS showed no indication of Re concentration fluctuations in the $KReO_4$ glass, whereas the Re_2O_7 glass showed evident inclusions by LA-ICP-MS (Fig. 8). It is unclear at present why the reactivity and resultant crystallinity of the Re_2O_7 glass is different, but it may be related to the segregation and interaction with a sulfate phase (Fig. 5).

- The significant spread in the values of retained Re concentration in glasses with target Re concentration > 6,500 ppm is due to the heterogeneous distribution of rhenium-rich inclusions in the glass matrix as has been already shown by XRD (Fig. 2).
- Some of the reduction in retention in the glass was due to formation of the white rhenium salt. Note that the salt layer was removed from the glass surface before analysing the glasses by ICP-OES and thus its Re content is not included in the soluble fraction of Re. The surface salts therefore represent a loss of retention of the target Re concentration.
- As is evident from Fig. 10, the retention ratio varied between 0.8 and 1 for glasses with target Re concentration ≤ 2,500 ppm while beyond that, R_i decreased considerably. The decreasing retention for low target Re concentrations can be attributed to volatility of rhenium from the glass melt and subsequent deposition on the walls of quartz ampoule. At higher Re target concentrations, Re salt could be lifted to the surface of the glass melt trapped in bubbles originating from the pores of the glass powder as it sinters or from redox reactions of Re or Fe. Tiny bubbles that remained in the glass after cooling were investigated by LA-ICP-MS. These bubbles did not contain Re (see **Supplementary Information**).

3.6 Redox and valence in Re and Tc

Although Re has been widely accepted as a surrogate for Tc, it is important to highlight some differences between the two species regarding their chemistry within the glass environment. Rhenium has a bulk silicate Earth abundance of 0.2 ppb and is the rarest of all the naturally occurring elements, apart from the noble gases,[24] thus there have been few comprehensive studies on its behavior outside of the geochemistry literature. The most prominent difference between Tc and Re is their contrasting reduction-oxidation (redox) behavior. Rhenium commonly occurs in the +7 oxidation state as Re_2O_7 or ReO_4^- (perrhenate ion) as well as in the +4 state in ReO_2 and the +6 state in ReO_3, whereas Tc occurs only in the 7+ or 4+ oxidation states.[8, 25]

Tc is more easily reduced from $Tc^{7+} \rightarrow Tc^{4+}$ compared to $Re^{7+} \rightarrow Re^{4+}$,[8] and thus it has been suggested that Re may not be a representative substitute for Tc under reducing conditions, at least in borosilicate LAW glasses.[12] In the vapor hydration test (VHT) used to assess chemical durability,[26] Tc has been observed to reduce to Tc^{4+} regardless of the starting Tc valence distribution, whereas Re^{7+} species remained dominant in the Re glass analogues.[27] Furthermore, Tc is enriched at the outer corroded gel-layer of amorphous silica while almost absent at the center, while Re concentrations are lower near the surface of comparable samples and approach that of unreacted glass near the center, thus highlighting the difference in mobility of Re and Tc in hydrothermal environments. Also, a series of recent melter tests suggest that the retention of Re is 8 to 10% higher than Tc for similar glasses.[28] Despite the lack of precise correlation in the redox of Re and Tc, the assumption of 100% Tc^{7+} and use of Re^{7+} as a surrogate should lead to a conservative estimate for solubility of Tc in an oxidizing environment, such as that present in the high nitrate feed environment at Hanford. Since Tc^{4+} is not nearly as mobile in water as Tc^{7+} (as

TcO_4^-) and not as volatile, the applicability of Re^{7+} data to Tc for these glasses should be reasonable. However, it should not be assumed that the solubility of Tc^{4+} (or Re^{4+}), which may be present in non-negligible quantities in other nuclear waste glasses, would be the same as the solubility of Tc^{7+} (or Re^{7+}).

According to the literature, volatility and retention of Tc and Re compounds in silicate and borosilicate glasses is strongly dependent on the oxidation state of the glass as well as on the feed chemistry.[8, 12] For example, Tc and Re tend to be more volatile when present as Tc^{7+}/Re^{7+} (TcO_4^-/ReO_4^-) than when present as Tc^{4+}/Re^{4+} (TcO_2/ReO_2). On the other hand, $KTcO_4$ and $KReO_4$ precursors are expected to produce lower Tc and Re volatilization at higher temperatures compared to Tc_2O_7 and Re_2O_7, respectively.[8, 29] Thus, the calculated or predicted maximum content of Tc/Re in glass in these literature studies is not the *solubility* but, rather, is the *retention* of Tc/Re in the glass after volatilization of these species during melting, the value of which should be significantly lower than the true solubility.

A number of studies have focused on the Tc or Re valences and concentrations in silicate or borosilicate glasses synthesized under various conditions, in order to determine the effect of the Tc/Re source starting material and redox on the solubility, retention, and volatility in glass.[12, 30-32] While the results from most of these studies seem to contradict each other, they actually provide a coherent description of the behavior of Re in silicate melts. Initial studies by O'Neill *et al.*[30] and Righter and Drake[31] suggested that Re dissolves in silicate melts as species with unusually low, valence states (Re^+ or Re^{2+}). Later work by Ertel *et al.*[32] demonstrated that these results were due to the presence of metallic Re "micronuggets" dispersed in the silicate melt. Using LA-ICP-MS, Ertl *et al.*[32] showed that Re actually dissolved in silicate melts with oxygen fugacities lower than 10^{-8} bar was present as Re^{4+} and Re^{6+}, but these species were only present

at 0.03 ppm concentrations in the presence of roughly 20 ppm of metallic Re. These results are consistent with those of Lukens *et al.*,[12] which spanned a much wider range of oxygen fugacities. At low oxygen fugacities, only metallic Re was observed in cooled glass samples, while at higher oxygen fugacities only Re^{7+} was observed[12] (XANES used in the cited study is not sensitive to the presence of small amounts of either Re^{4+} or Re^{6+} in the presence of a large excess of metallic Re or Re^{7+}).

The initial motivation for examining our samples using LA-ICP-MS were the previous reports that Re could concentrate in reduced metallic form in "micronuggets" in silicate melts which would skew the assessed solubility of a glass containing them.[32] Other than the evidence of inclusions, most probably sodium and potassium perrhenate, we did not see any evidence of the metallic "micronuggets" causing small but measurable fluctuations in Re concentration suggested by these previous authors, though these would be less likely to occur in our samples due to the specific redox conditions. Inclusions containing Re in our samples were indicated by very large excursions of Re concentration and were very spatially confined, which is phenomenologically different than the heterogeneous Re distribution reported by the geochemists.

An estimate for the solubility of Tc in borosilicate glass might be made based on a comparison of the solubility of Re measured in this study with the solubility of sulfur in borosilicate glass measured in various studies (~0.6 mol% SO_3 or ~3,000 ppm by mass S).[33] Using this value for sulfur solubility, the ppm mass value can be converted to a parts per million atoms (ppma) basis, and for the sodium borosilicate LAW glass with composition studied here, this equates to ~1,900 ppma for sulfur. The equivalent value for Re in our LAW glass assuming 3,000 ppm by mass solubility is ~333 ppma for rhenium, which is a six-fold reduction in

solubility compared to sulfur. One might speculate that this decreased solubility for Re compared to S, neither of which appear to participate in the glass network, is due to the much larger ionic radius of Re (S^{6+} = 43 pm, Re^{7+} = 67 pm, Tc^{7+} = 70 pm [34]). By this argument, then, Tc^{7+} should have an equivalent slightly lower solubility (in ppma) than Re^{7+}. Assuming the same ~333 ppma solubility for Tc^{7+} in this glass, its solubility should be ~1,500 ppm by mass.

From the standpoint of ultimate disposition of radioactive Tc in a glass waste form, a few considerations should be made. The required average maximum concentration of Tc to be immobilized in Hanford LAW glass can be estimated from 1) the estimated total Tc inventory in the underground tanks (~1,500 kg per Mann 2004[2]) and 2) the total estimated mass of LAW glass to be produced (527,838 metric tons per Certa et al 2011[1]). Assuming 100% retention of Tc and these numbers, the average Tc concentration in LAW glass is ~3 ppm by mass. Assuming that the solubility of Tc^{7+} on a per atom basis in glass is similar to that obtained for Re^{7+}, and assuming the redox state in LAW glass favors Tc^{7+}, solubility of Tc is orders of magnitude higher than current estimates of Tc concentrations in LAW, even when recycle loops are taken into account which theoretically ultimately result in 100% retention for volatile species. On the other hand, the apparent solubility of Re^{4+} in glass appears to be very low,[32] and if the same is true for Tc^{4+}, then the solubility of Tc in silicate glass depends greatly on the redox state of the melt. Additionally, as previously stated, Tc^{7+} is much more easily reduced than Re^{7+}, so Tc^{4+} may indeed be present in non-negligible concentrations in LAW glass, a possibility which should be verified experimentally. If Tc^{4+} is present in significant quantities, the solubility data obtained in the literature for Re^{4+} may not be relevant for Tc^{4+} since Re^{4+} is so difficult to form in realistic glass compositions, and another surrogate should be considered, such as Ti^{4+}, or preferably Ru^{4+}.[35] In Tc^{4+} the *d*-electrons are anti-bonding, which weakens the interaction

between oxide ligands and the metal, a situation more closely replicated by Ru which is adjacent to Tc on the periodic table. However, it is likely that Tc^{7+} will be the most important Tc valence for Hanford LAW glass due to the decomposition of nitrate and thus highly oxidizing environment in the melter.

The more important issue, then, becomes Tc retention. As shown by this study with Re, the retention can be substantially lower than the solubility even at low target concentrations due to kinetic factors such as volatility. Here future work will be needed to understand the details of the interaction between formation of a low-melting salt phase in LAW glass (which may contain pertechnetate, sulfate, chromate, chloride, iodide, nitrate, and nitrite along with various alkali metals), and volatilization from the cold cap where the slurry feed comes in contact with the melt pool. Here, previous work has shown that despite the estimated solubility of sulfate in borosilicate glass (~0.6 mol%), salt formation occurs at lower sulfate concentrations than its solubility.[36] Additionally, despite low concentrations of ^{137}Cs in LAW, which are less than that estimated for pertechnetate as most ^{137}Cs is partitioned to HLW, pertechnetate has been shown to enhance the volatility (and hence reduce the retention) of Cs,[8] possibly due to the formation of volatile $CsTcO_4$, resulting in additional safety concerns about the uncontrolled release of this short half-life, high dose contributor. Controlling the redox of the cold cap, then, to prevent formation of Tc^{7+} (and thus TcO_4^-) has been an area of intense research; however, decomposition of nitrites during vitrification of LAW glass will create highly oxidizing conditions in the melt, which may result in the formation of Tc^{7+} regardless of the initial oxidation state.[37]

4. Conclusions

We have determined that the solubility of rhenium in Na_2O-Al_2O_3-B_2O_3-SiO_2 simulated nuclear waste glass is ~3,000 ppm by mass when glass is equilibrated at 1000 °C for the

particular composition studied, a high sodium borosilicate representative of Hanford Low Activity Waste (LAW) glass. In all the glasses studied, the primary Re valence was +7, with a possible small fraction (<10%) of +4 in the glass when the maximum target of $KReO_4$ was added to the frit. We expect the solubility of Tc^{+7} to be substantially similar to that shown for Re^{+7} in this study, and a reduced scope test program is underway to verify this hypothesis. Given the high solubility of Re (and presumably Tc) in borosilicate glass, it is concluded that solubility is not a limiting factor in processing nuclear waste into glass given the currently estimated scenarios. Rather, it is the retention in glass that is the bigger concern, which is a more complex kinetic problem involving volatilization, phase separation, and complexation with alkali in the cold cap.

5. Acknowledgements

This work was supported by the Department of Energy – Waste Treatment & Immobilization Plant (WTP) Federal Project Engineering Division. The authors thank Orville (Tom) Farmer III for consultation regarding LA-ICP-MS, Prof. J.M.F. Ferreira from University of Aveiro, Portugal for FTIR and MAS-NMR, Juan (Jenny) Liu for EPMA-WDS, Charles Windisch, Jr., for Raman spectroscopy, and Jaehun Chun for comments on the manuscript. Pacific Northwest National Laboratory is operated by Battelle Memorial Institute for the U.S. Department of Energy under contract DE-AC05-76RL01830. Portions of this work were supported by U.S. Department of Energy, Basic Energy Sciences, Chemical Sciences, Biosciences, and Geosciences Division, Heavy Element Chemistry Program and were performed at Lawrence Berkeley National Laboratory under Contract No. DE-AC02-05CH11231. Portions of this research were carried out at the Stanford Synchrotron Radiation Lightsource, a

Directorate of SLAC National Accelerator Laboratory and an Office of Science User Facility operated for the U.S. Department of Energy Office of Science by Stanford University.

References

1. P. J. Certa and P. A. Empey, River Protection Project System Plan, ORP-11242 Revision 6, Office of River Protection, US Department of Energy, Richland, WA, 2011.
2. F. Mann, Annual Summary of the Integrated Facility Performance Assessment for 2004, DOE/ORP-2000-19 Revision 4, CH2M HILL Hanford Group, Inc., Richland, WA, 2004.
3. J. H. Westsik, Hanford site secondary waste roadmap, PNNL-18196, Pacific Northwest National Laboratory, Richland, WA, 2009.
4. F. M. Mann and R. E. Raymond, Risk analysis supporting the decision of the initial selection of supplemental ILAW technologies, RPP-17675, Rev. 0, CH2M Hill Hanford Group, Richland, WA, 2003.
5. G. Shaw, ed., *Radioactivity in the terrestrial environment*, Elsevier, Oxford, UK, 2007.
6. W. Um, H.-S. Chang, J. P. Icenhower, W. W. Lukens, R. J. Serne, N. P. Qafoku, J. H. Westsik, E. C. Buck and S. C. Smith, *Environ. Sci. Technol.*, 2011, **45**, 4904-4913.
7. H. Lammertz, E. Merz and S. Halaszovich, *Mat. Res. Soc. Symp. Proc.*, 1985, **44**, 823-829.
8. J. G. Darab and P. A. Smith, *Chem. Mater.*, 1996, **8**, 1004-1021.
9. K. S. Matlack, I. S. Muller, I. L. Pegg and I. Joseph, Improved Technetium Retention in Hanford LAW Glass - Phase 1, VSL-10R1920-1, Vitreous State Laboratory, The Catholic University of America, Washington, DC, 2010.
10. D. S. Kim, L. M. Bagaasen, J. V. Crum, A. Fluegel, A. Gallegos, B. Martinez, J. Matyas, P. A. Meyer, D. R. Paulsen, B. J. Riley, M. J. Schweiger, C. W. Stewart, R. G. Swoboda and J. D. Yeager, Investigation of Tc migration mechanism during bulk vitrification process using Re surrogate, PNNL-16267, Pacific Northwest National Laboratory, Richland, WA, 2006.

11. D. S. Kim, C. Z. Soderquist, J. P. Icenhower, B. P. McGrail, R. D. Scheele, B. K. McNamara, L. M. Bagaasen, M. J. Schweiger, J. V. Crum, J. D. Yeager, J. Matyas, L. P. Darnell, H. T. Schaef, A. T. Owen, A. E. Kozelisky, L. A. Snow and M. J. Steele, Tc reductant chemistry and crucible melting studies with simulated Hanford Low-Activity Waste, PNNL-15131, Pacific Northwest National Laboratory, Richland, WA, 2005.

12. W. W. Lukens, D. A. McKeown, A. C. Buechele, I. S. Muller, D. K. Shuh and I. L. Pegg, *Chem. Mater.*, 2007, **19**, 559-566.

13. A. F. Armstrong and J. F. Valliant, *Dalton Trans.*, 2010, **39**, 8128-8131.

14. J. R. Dilworth and S. J. Parrott, *Chem. Soc. Rev.*, 1998, **27**, 43-55.

15. A. J. West, *Annu. Rep. Prog. Chem., Sect. A: Inorg. Chem.*, 2011, **107**, 173-182.

16. F. A. Cotton and G. Wilkinson, *Advanced Inorganic Chemistry*, John Wiley & Sons, New York, 1980.

17. D. C. Koningsberger and R. Prins, *X-Ray Absorption: Principles, Applications, Techniques of EXAFS, SEXAFS, and XANES*, John Wiley & Sons, New York, 1988.

18. B. Ravel and M. Newville, *Phys. Scripta*, 2005, **T115**, 1007-1010.

19. SIXPack (Sam's Interface for XAS Package) Documentation, http://ssrl.slac.stanford.edu/~swebb/spdocs/sixpack_documentation.htm.

20. K. P. Jochum, U. Weis, B. Stoll, D. Kuzmin, Q. Yang, I. Raczek, D. E. Jacob, A. Stracke, K. Birbaum, D. A. Frick, D. Günther and J. Enzweiler, *Geostand. Geoanal. Res.*, 2011, **35**, 397-429.

21. P. J. Sylvester and S. M. Eggins, *Geostand. Newslett.*, 1997, **21**, 215-229.

22. S. F. Durrant, *J. Anal. Atom. Spec.*, 1999, **14**, 1385-1403.

23. P. Hrma, Retention of halogens in waste glass, PNNL-19361, Pacific Northwest National Laboratory, Richland, WA, 2010.

24. H. S. C. O'Neill and H. Palme, *Composition of the silicate Earth: Implications for accretion and core formation. In The Earth's Mantle: Composition, Structure and Evolution*, Cambridge University Press, Cambridge, U.K., 1999.

25. J. M. MacKenzie and D. Canil, *Geochim. Cosmochim. Acta*, 2006, **70**, 5236-5245.

26. ASTM C 1663-09, *Standard test method for measuring waste glass or glass ceramic durability by vapor hydration test*, ASTM International, West Conshohocken, PA.

27. D. A. McKeown, A. C. Buechele, W. W. Lukens, D. K. Shuh and I. L. Pegg, *Environ. Sci. Technol.*, 2006, **41**, 431-436.

28. K. S. Matlack, I. S. Muller, R. A. Callow, N. D'Angelo, T. Bardacki, I. Joseph and I. L. Pegg, Improved technetium retention in Hanford LAW Glass-Phase 2, VSL-101R2260-1, Vitreous State Laboratory, The Catholic University of America, Washington, DC, 2011.

29. K. Schwochau, *Radiochim. Acta*, 1983, **32**, 139-152.

30. H. S. C. O'Neill, D. B. Dingwell, A. Borisov, B. Spettel and H. Palme, *Chem. Geol.*, 1995, **120**, 255-273.

31. K. Righter and M. J. Drake, *Earth Planet. Sci. Lett.*, 1997, **146**, 541-553.

32. W. Ertel, H. S. C. O'Neill, P. J. Sylvester, D. B. Dingwell and B. Spettel, *Geochim. Cosmochim. Acta*, 2001, **65**, 2161-2170.

33. R. K. Mishra, K. V. Sudarsan, P. Sengupta, R. K. Vatsa, A. K. Tyagi, C. P. Kaushik, D. Das and K. Raj, *J. Am. Ceram. Soc.*, 2008, **91**, 3903-3907.

34. R. D. Shannon, *Acta Crystallog. A*, 1976, **32**, 751-767.

35. H. D. Schreiber, F. A. Settle Jr, P. L. Jamison, J. P. Eckenrode and G. W. Headley, *JLCM*, 1986, **115**, 145-154.

36. J. D. Vienna, P. Hrma, W. C. Buchmiller and J. S. Ricklefs, Preliminary investigations of sulfur loading in Hanford LAW glass, PNNL-14649, Pacific Northwest National Laboratory, Richland, WA, USA, 2004.

37. P. A. Smith, J. D. Vienna and P. Hrma, *J. Mater. Res.*, 1995, **10**, 2137-2149.